

Comparing Tests for Near-Grazing-Incidence Noise Reduction and Sound Absorption Tests for Hot-Mix Asphalt

Tyler Dare, Wubeshet Woldemariam, Rebecca S. McDaniel, Jan Olek, and Robert Bernhard

Sound absorption measurements have been used as a simple, cost-effective way of assessing pavement noise properties in the laboratory. However, tire–pavement noise (TPN) is emitted close to the pavement at shallow angles of incidence between the tire and a roadside receiver. Absorption properties can be used to predict oblique incidence noise properties, provided that certain assumptions are met. Near-grazing-incidence predictions of noise vary widely, and the assumptions involved may not be applicable to porous asphalt pavements. A method of directly measuring near-grazing-incidence noise reduction of hot-mix asphalt pavements was designed. It was found that the results of the proposed test could not be predicted from absorption data alone except for dense-graded pavement. For porous or thin, gap-graded pavements, the near-grazing-incidence test gave additional useful information about the acoustic performance of the pavement samples. The test can be used to supplement absorption and other laboratory tests for more accurate predictions of TPN.

There is currently no way of accurately predicting tire–pavement noise (TPN) for hot-mix asphalt (HMA) pavements without constructing test pavements in the field. Because of the costs associated with constructing experimental field sections, laboratory tests of noise reduction properties of HMA are necessary. Though these tests cannot accurately account for all known mechanisms of TPN generation and propagation, the tests can be useful in determining which HMA mix designs should be selected for field testing.

One commonly used laboratory test of HMA noise properties is a normal incidence sound absorption test. As described in ASTM E1050, core samples from pavements in the field or laboratory specimens are placed in an impedance tube, and sound absorption is measured. Nondestructive alternatives to this standard have been developed involving an impedance tube placed flush against the pavement to be tested (1). Tests of normal incidence sound absorption have been used in models to predict TPN from pavement parameters (2–4).

T. Dare, Ray W. Herrick Laboratories, Office 76, 140 South Martin Jischke Drive, W. Woldemariam and J. Olek, School of Civil Engineering, Purdue University, 550 Stadium Mall Drive, West Lafayette, IN 47907. R. S. McDaniel, North Central Superpave Center, 1205 Montgomery Street, P.O. Box 2382, West Lafayette, IN 47906. R. Bernhard, University of Notre Dame, 510 Main Building, Notre Dame, IN 46556. Corresponding author: W. Woldemariam, wwoldema@purdue.edu.

Transportation Research Record: Journal of the Transportation Research Board, No. 2270, Transportation Research Board of the National Academies, Washington, D.C., 2012, pp. 1–8.
DOI: 10.3141/2270-01

However, normal incidence properties of pavement are not sufficient for quantifying a pavement's effect on TPN.

TPN sources are located close to the contact patch (5), so the angle at which sound reflects off the pavement to a receiver at the roadside is close to grazing. Near-grazing-incidence properties are also important for comparing the sound measured at the tire–road interface by using methods such as onboard sound intensity (AASHTO TP 76-11) with sound measured at the roadside using methods such as statistical pass-by (ISO 11819-1). Previous studies have been successful in comparing the two measurement types, but only when the surface between the road and wayside receiver is acoustically hard (6). However, Donovan recently used a loudspeaker and microphone configuration to demonstrate that differences between onboard sound intensity and pass-by results for porous pavements can be partially explained by differences in sound propagation over the pavement surfaces (7).

Near-grazing-incidence properties can be predicted from normal incidence tests based on certain simple models of sound reflection and absorption. These model-based predictions vary widely at angles approaching grazing incidence as near-grazing reflection and absorption are highly sensitive to the assumptions made in these models (8). Furthermore, the assumptions involved in predicting near-grazing-incidence properties from normal incidence tests are not generally true for situations in which sound can travel through a surface, such as HMA pavements constructed with one or more porous layers. Laboratory testing of near-grazing-incidence properties of HMA pavements is necessary to supplement standard normal incidence tests.

An experiment was designed for the measurement of near-grazing-incidence noise reduction on HMA pavements. In the test, a sound source is placed near a rectangular sample of HMA pavement and the subsequent sound field is measured. The source and microphone are positioned so that there is a shallow angle of incidence of the reflected sound. The results can be used to identify pavement designs with superior near-grazing-incidence noise reduction. Together with other laboratory tests, the near-grazing-incidence noise reduction test can be used to identify pavements likely to have reduced TPN in the field.

Thin, gap-graded (TG) pavement surfaces are asphalt mixtures that are typically laid to a thickness between 20 mm and 40 mm. TG surfaces have noise-reducing properties due partly to the small aggregate size, which helps to reduce noise generated by irregularities in the surface texture. TG surfaces also have negative texture; that is, the texture is composed of voids that generally lie below the upper flat surface plane on which the vehicle travels. TG surfaces

tend to allow only a low level of TPN generation since the negative texture suppresses the shock or vibration mechanism. Gap-grading also gives the surfaces good porosity, which helps to reduce noise generated by air pumping (9).

Porous asphalt surfaces contain a high volume of voids (as much as 28% at the time of placement), which are open and interconnected for improved water circulation and absorption of surface noise. The high percentage of voids is achieved by using a very high content of aggregates greater than 2 mm in size (83% to 87%). As a wearing course, the layer thickness is typically about 40 mm (9).

Porous asphalt can be constructed as a two-layer pavement. Single-layer porous (SLP) asphalt reduces noise more than conventional dense asphalt concrete (9). Double-layer porous (DLP) asphalt has been used primarily to avoid clogging on urban roads and hence provide acoustic durability. This property is caused by using the upper layer as a sieve for dirt and debris and the bottom layer to provide wide channels to collect the dirt finer than the pores of the top layer (10).

PURPOSE AND SCOPE OF STUDY

The purpose of this study was to illustrate when the near-grazing-incidence noise reduction test gives different information to researchers than would be predicted from normal incidence absorption testing and model predictions.

Different TG, SLP, and DLP specimen types that varied in their mixture and cross-sectional parameters such as design air void content (V_a), nominal maximum aggregate size (NMAS), binder type, slab thickness, and aggregate type were prepared in the laboratory, along with one dense-graded asphalt sample. After near-grazing-

incidence noise reduction tests were conducted on all of the samples, core samples were taken from each specimen and normal incidence sound absorption was measured. The results of the near-grazing-incidence test were compared with predictions from the standard sound absorption test to determine for which pavement types the near-grazing-incidence test can give additional information to pavement designers.

SPECIMEN TYPES

TG, SLP, and DLP Specimens

TG, SLP, and DLP specimen types considered in the current study are shown in Table 1. The TG, SLP, and DLP specimens shown in Table 1 differ in their mixture parameters. As shown, four levels of target V_a void content were considered: 10%, 20%, 30%, and 40%. Three levels of NMAS were used: 4.75 mm, 9.5 mm, and 12.5 mm. Two types of binder were used: PG 64-22 (unmodified binder) and PG 76-22 (modified binder). Aggregate types used in the study were granite, expanded shale, steel slag, and dolomite. Five types of gradations (based on NMAS and whether the mixture is porous or gap-graded) were considered: 4.75-mm porous surface mix (PSM), 4.75-mm gap-graded surface mix, 9.5-mm PSM, 12.5-mm PSM, and 12.5-mm gap-graded surface mix. The mixture gradation is shown Figure 1.

The TG, SLP, and DLP specimen slabs were 1016 mm long, 508 mm wide, and of variable thickness, depending on the type of specimen shown in Table 1. The dimensions were chosen so that the samples would be maneuverable in the laboratory and so that there would be an adequate frequency range of the noise results,

TABLE 1 Types of TG, SLP, and DLP Specimens

| Parameter | Level | Specimen Type | | | | | | | | | | | |
|----------------|--------------------|------------------|------|------|------|------|------|------|------|---------------------|-------|-------|-------|
| | | Thin, Gap-Graded | | | | | | | | Single-Layer Porous | | | |
| | | TG-1 | TG-2 | TG-3 | TG-4 | TG-5 | TG-6 | TG-7 | TG-8 | SLP-1 | SLP-2 | SLP-3 | SLP-4 |
| Air void (%) | 10 | ✓ | — | — | — | — | — | — | — | — | — | — | — |
| | 20 | — | ✓ | ✓ | ✓ | ✓ | ✓ | ✓ | ✓ | ✓ | — | — | — |
| | 30 | — | — | — | — | — | — | — | — | — | ✓ | ✓ | ✓ |
| | 40 | — | — | — | — | — | — | — | — | — | — | — | — |
| NMAS (mm) | 4.75 | ✓ | ✓ | — | — | — | — | — | — | ✓ | ✓ | — | — |
| | 9.5 | — | — | ✓ | ✓ | ✓ | ✓ | ✓ | ✓ | — | — | ✓ | ✓ |
| | 12.5 | — | — | — | — | — | — | — | — | — | — | — | — |
| Binder grade | PG 64-22 | ✓ | ✓ | ✓ | — | — | — | — | — | ✓ | ✓ | ✓ | — |
| | PG 76-22 | — | — | — | ✓ | ✓ | ✓ | ✓ | ✓ | — | — | — | ✓ |
| Thickness (mm) | 20 | ✓ | ✓ | ✓ | ✓ | — | — | — | — | — | — | — | — |
| | 40 | — | — | — | — | ✓ | ✓ | ✓ | ✓ | ✓ | ✓ | ✓ | ✓ |
| | 50 | — | — | — | — | — | — | — | — | — | — | — | — |
| Aggregate | Granite | — | — | — | — | — | ✓ | — | — | — | — | — | — |
| | Dolomite | ✓ | ✓ | ✓ | ✓ | ✓ | — | — | — | ✓ | ✓ | ✓ | ✓ |
| | Steel slag | — | — | — | — | — | — | ✓ | — | — | — | — | — |
| | Steel slag (85%) + | — | — | — | — | — | — | — | ✓ | — | — | — | — |
| | Exp. shale (15%) | — | — | — | — | — | — | — | — | — | — | — | — |

NOTE: Check mark (✓) = at selected level, given parameter is considered for given specimen type; — = at selected level, given parameter is not considered for given specimen type; TG = thin, gap-graded asphalt specimen; SLP = single-layer porous specimen; DLP = double-layer porous specimen; TG-1, TG-2, TG-3, TG-4, TG-5, TG-6, TG-7, TG-8 = thin, gap-graded asphalt specimen types 1, 2, 3, 4, 5, 6, 7, and 8, respectively; SLP-1, SLP-2, SLP-3, SLP-4, SLP-5, SLP-6, SLP-7, SLP-8, SLP-9 = single-layer porous specimen types 1, 2, 3, 4, 5, 6, 7, 8, and 9, respectively; DLP-1, DLP-2, DLP-3, DLP-4, DLP-5, DLP-6, DLP-7, DLP-8, DLP-9 = double-layer porous specimen types 1, 2, 3, 4, 5, 6, 7, 8, and 9, respectively; TL = top layer; BL = bottom layer; exp. = expanded.

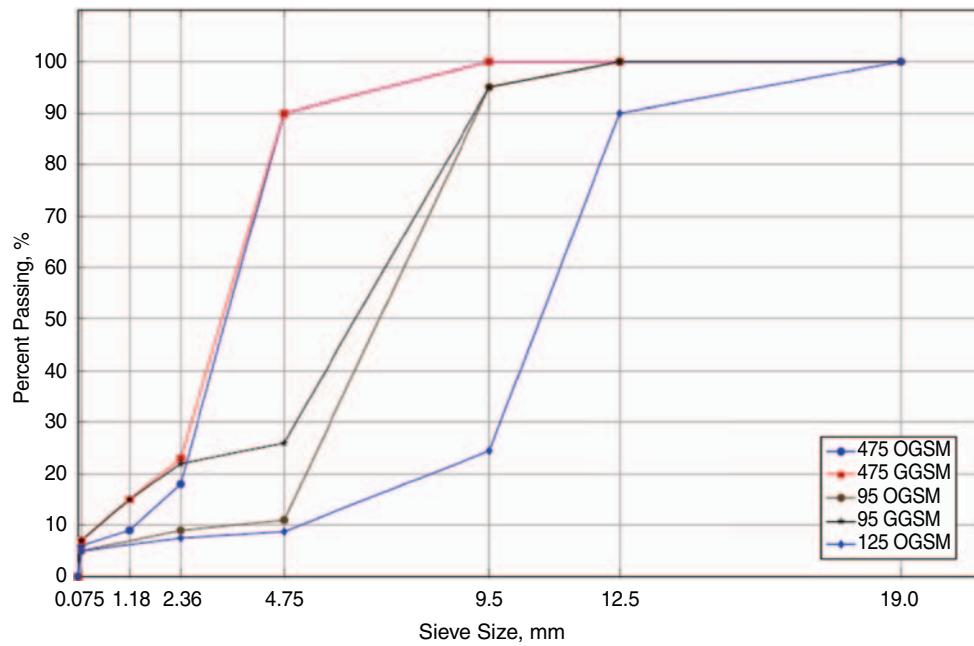


FIGURE 1 Mixture gradations used (OGSM = open-graded surface mix; GGSM = gap-graded surface mix).

as will be described. A typical HMA slab is shown in Figure 2. The specimens were compacted in wooden frames, and the top of the sides of each frame was at the same level as the top of the HMA. Recent research by Rochat and Read (11) has shown that differences in the pavement layer beneath thin porous surfaces can affect noise propagation measurements. For this research, the

HMA samples were backed by plywood, which is acoustically reflective, similar to the backing in the impedance tube tests described later. A dense-graded asphalt slab specimen with 9.5-mm nominal maximum aggregate size and 7% air void content was prepared to compare its acoustic performance with that of the TG, SLP, and DLP specimens.

[illegible]

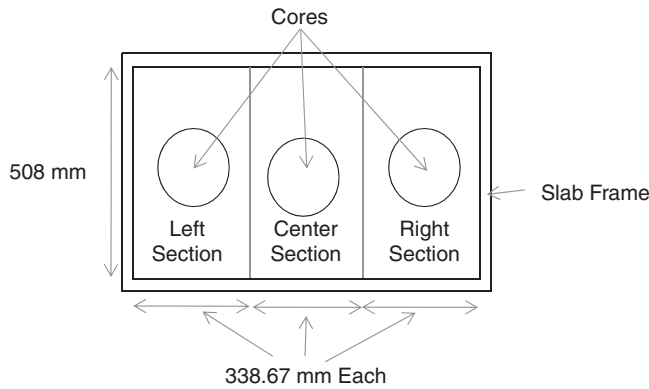


FIGURE 2 Locations of core samples taken from HMA specimens (figure not drawn to scale).

Wood Specimen

A final sample was constructed out of plywood. The plywood sample had the same dimensions as the HMA specimens and was 19 mm thick. The wood sample was tested with the same procedures for both the near-grazing-incidence test and the sound absorption test. The plywood specimen was used to demonstrate results for an acoustically reflecting surface for which predictions of near-grazing-incidence noise characteristics can be made from normal incidence measurements.

Impedance Tube Test Samples

Impedance tube test samples were cored from the HMA slabs with a 100-mm (4-in.) diameter core drill. Three representative impedance tube test samples were cored from each HMA slab in the laboratory. Samples were cored from the left section, center section, and right section of each HMA slab, as shown in Figure 2. The absorption properties of each slab were determined by averaging the absorption properties of the three core samples taken from the slab.

TEST FOR NEAR-GRAZING-INCIDENCE NOISE REDUCTION

Test Setup

The near-grazing-incidence test setup is shown in Figures 3 and 4. The microphone and sound source were placed 10 cm from the

specimen. The microphone was a Brüel and Kjær Type 4192 and the sound source consisted of a loudspeaker attached to a tube 1 m long and approximated a point monopole. The source and microphone were spaced 80 cm apart and 40 cm from the center of the specimen. The angle of incidence was approximately 76 degrees from normal incidence (14 degrees from grazing incidence). Both the sound source and microphone were connected to a Brüel and Kjær Type 3109 input-output module and Type 7533 LAN interface module. White noise was generated by the input-output module and passed through an amplifier to drive the sound source. The noise field was then measured by the microphone at a sample rate of 16,384 Hz. Data from the microphone were recorded as unweighted, 10-s-long time histories. In addition, the voltage output of the amplifier was recorded to ensure constant noise output from the sound source. Measurements were taken on all specimens. Additional measurements were taken without any specimen in place, which is referred to here as the anechoic condition.

Data Analysis

Ten seconds' worth of sound pressure data was measured for each specimen and for the anechoic condition. Each time history was separated into 40 smaller time histories, each 0.25 s long. Calculations were made by using each of the smaller time histories, and the results were averaged.

Each time history was multiplied by a Hann window, and the discrete Fourier transform was taken to calculate the narrow-band, complex sound pressure spectrum. For comparison purposes, the sound pressure spectrum for an ideal, perfectly reflecting surface was calculated. The anechoic sound pressure spectrum was used to calculate the theoretical perfectly reflecting spectrum:

$$P_R = P_A \left(1 + \frac{r_1}{r_2} e^{jk(r_1 - r_2)} \right) \quad (1)$$

where

P_R = sound pressure spectrum expected for infinite, perfectly reflecting surface;

P_A = complex sound pressure spectrum measured in anechoic condition;

r_1 = 80.0 cm = length of direct path from sound source to microphone;

r_2 = 82.5 cm = length of reflected path; and

$j = \sqrt{-1}$.

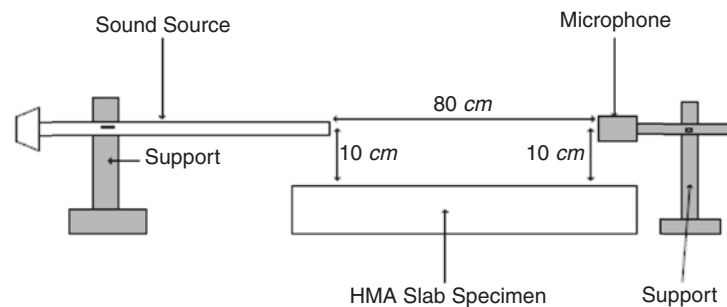


FIGURE 3 Schematic of near-grazing-incidence test setup.

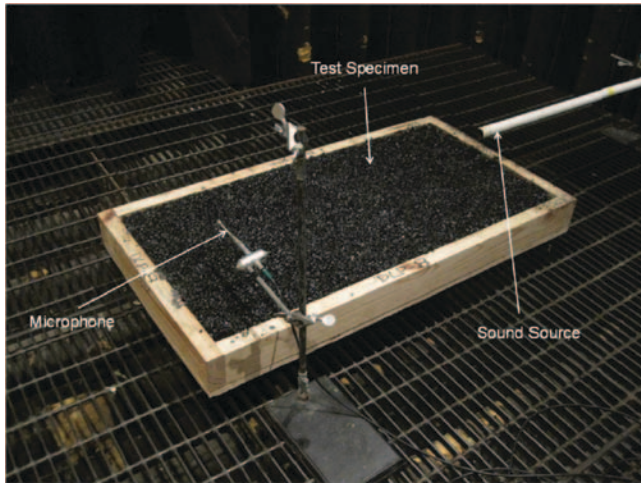


FIGURE 4 Near-grazing-incidence test setup.

The value of k is defined as follows:

$$k = \frac{2\pi f}{c} \quad (2)$$

where f is the frequency in hertz and $c = 343$ m/s is the speed of sound in air. P_R was calculated for each of the 40 small time histories in the anechoic condition. The magnitude of each P_R was calculated and the results were averaged to calculate the average sound pressure spectrum for an ideal reflecting surface.

The sound pressure spectrum for each of the HMA surfaces, P_S , was also measured. One-twelfth-octave band spectra were calculated from narrow-band spectra by taking the average sound pressure in each band. The sound reduction properties of each HMA sample were then calculated:

$$L_S = 20 \log_{10} \frac{P_S}{P_R} \quad (3)$$

where L_S represents the excess near-grazing-incidence noise of a given surface compared with that of an ideal reflecting surface. Negative values of L_S indicate that the test surface reflects less sound and therefore is quieter than an ideal reflecting surface. No asphalt surface would typically reflect more sound than an ideal reflecting surface. Thus, L_S would not normally be greater than zero decibels. The exception would be cases in which the reflected sound and the direct sound are in phase so that they reinforce each other.

The low-frequency limit for the test was determined by the frequency with wavelength equal to the smallest dimension of the test sample. For this test, the smallest dimension was 508 mm, and the low-frequency limit was approximately 675 Hz. The high-frequency limit was determined by the size of the largest features in the pavement. The highest valid frequency is that in which the wavelength is approximately 10 times longer than that of the largest pavement feature. At frequencies higher than this limit, sound may be scattered instead of reflected at the interface. For this test, the largest top-layer aggregate was 9.5 mm, giving a high-frequency limit of approximately 3,600 Hz. Since fractional-octave band measurements were used, the frequency range was rounded down to the next one-third octave band, giving a valid frequency range of 800 to 3,200 Hz for the near-grazing-incidence test.

TEST FOR NORMAL INCIDENCE SOUND ABSORPTION

Acoustic absorption of the HMA and wood cores was measured according to ASTM E1050-10. An impedance tube, two microphones, and a digital frequency analysis system were used to measure the normal incidence acoustic absorption. The equipment used for this test is shown in Figure 5. Each sample was placed into the testing section of the tube (white area, Figure 5) and a rigid back was placed flush with the bottom of the test sample. For each sample, the edge closer to the microphones was sealed with clay to prevent leakage around the samples. For each slab, the absorption spectra for each of the three cores were averaged to get an average absorption spectrum for each pavement specimen. The diameter of the tube was 100 mm, making the high-frequency limit for the absorption data approximately 1,600 Hz.

Predictions of the near-grazing-incidence noise reduction were made from the measured normal incidence absorption spectra for comparison with measured results by using a simple, locally reacting acoustical model. The model assumes that the reflection coefficient is real and that it is the same at all angles of incidence. For the predictions, each pavement was assumed to be a locally reacting surface, meaning that reflection at a point on the surface is dependent only on the acoustical properties at that point on the surface. The sound pressure spectrum predicted from each surface is given as follows:

$$P'_S = P_A \left[1 + \sqrt{1 - \alpha} \frac{r_1}{r_2} e^{jk(r_1 - r_2)} \right] \quad (4)$$

where P'_S is the predicted sound pressure spectrum for the near-grazing-incidence test and α is the measured sound absorption. The predicted excess near-grazing-incidence noise is defined by

$$L'_S = 20 \log_{10} \frac{P'_S}{P_R} \quad (5)$$

where L'_S is the predicted excess near-grazing-incidence noise spectrum, calculated as both narrow-band and one-twelfth-octave bands



FIGURE 5 Impedance tube in test for normal incidence acoustic absorption.

as described previously. L'_S was then compared with L_S , the measured excess near-grazing-incidence noise spectrum, to determine if the reflection coefficient measured with the near-grazing-incidence test and the reflection coefficient measured with the normal incidence absorption test and the locally reactive acoustics model give equivalent results.

RESULTS

An example of typical narrow-band results is shown in Figure 6. For this plot, 0 dB represents the noise level for a perfectly reflecting surface, and negative values represent a reduction in noise compared with that from a reflecting surface. The spectrum predicted with the absorption data (dotted black curve) is close to 0 dB across most of its valid frequency range. This spectrum dips down to -5 dB around 1,000 Hz, corresponding to an increase in the measured sound absorption spectrum at this frequency. Thus, except for the frequency band around 1,000 Hz where the normal incidence absorption is significant, this pavement sample would be expected to behave like an ideal reflecting surface.

The measured spectrum (gray curve) has a dip around 1,350 Hz, and the reduction is about 25 dB from that of a perfectly reflecting surface. On this plot, a perfectly absorbing pavement would yield about -6 dB across the usable frequency range. Apparent noise reductions below this number, such as the ones seen at about 1,350 Hz, are due to interference between the direct and reflected waves. The frequency of the interference phenomenon depends on the difference in path length between the two waves. For locally reacting pavements with this microphone and source arrangement, this first noise reduction due to interference occurs at about 7,000 Hz. However, for extended-reaction pavements, such as porous asphalt, surface waves can exist so that the path length of the reflected wave is a function of the surface properties. Since the path-length difference depends on microphone location, the apparent dips in noise level cannot be used to make conclusions about noise properties at

wayside measurement distances. Analysis must be limited to frequencies at which there are no interference effects, characterized by sharp dips greater than 6 dB. Though the frequency ranges of the two tests only overlap in the 800- to 1,600-Hz range, it is clear that near-grazing-incidence results cannot be predicted from the normal incidence test for this pavement sample.

Typical results from samples of each of the HMA sample types tested are shown in Figure 7. The porous and TG samples (Figure 7, *a*, *b*, and *c*) share many of the same features. The measured excess noise spectra (gray curves) and the spectra predicted from absorption measurements (dotted black curves) show similarly shaped dips, but the dips are predicted to be at lower frequencies than those measured. In addition, the dips are much sharper in the measured case, indicating surface wave interference along with absorption effects. The results of some DLP samples, such as the one shown in Figure 7*b*, show that although the measurements qualitatively do not match predictions, there can still be a good fit between the two in the frequency range where the two tests overlap, between 800 Hz and 1,600 Hz. The results for the dense-graded asphalt sample are shown in Figure 7*d*. No dips in noise due to interference were measured, and there is a much better fit between the measured and predicted cases.

The average difference between the measured and predicted one-twelfth-octave band spectra is shown in Figure 8. The one-twelfth-octave band error is a better measure of the fit between the measured and predicted noise spectra, since TPN is usually expressed in fractional-octave bands. The frequency range for this analysis was limited to the range of overlap between the near-grazing-incidence test and the sound absorption test, between 800 Hz and 1,600 Hz. In general, the near-grazing-incidence measurements could not be predicted from absorption information for the porous or TG pavements. The results for the dense-graded asphalt and wood samples matched predictions within about 1 dB, and no sharp dips from interference were seen in the near-grazing-incidence results. Two of the DLP samples, DLP-7 and DLP-9, could be predicted within 1 dB, but qualitatively the shape of the spectra did not match, as shown in Figure 7*b*. Much of the difference between the measured

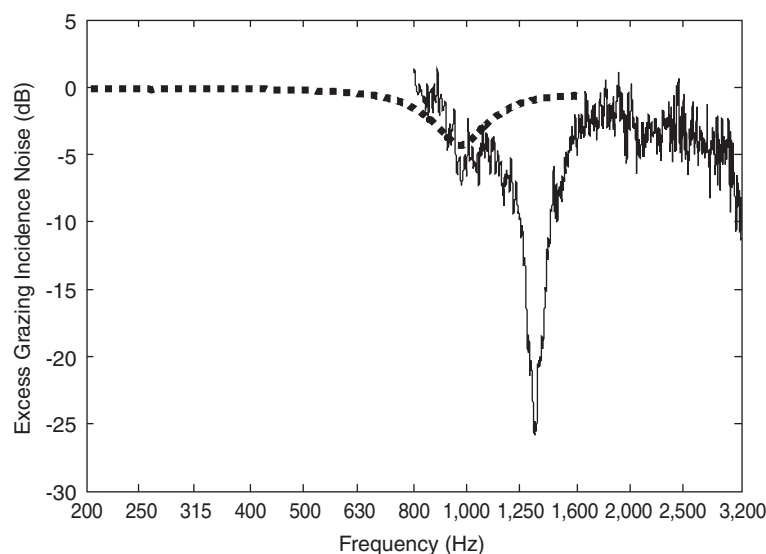


FIGURE 6 Narrow-band excess near-grazing-incidence noise spectra for Sample SLP-5 (dotted black curve: spectrum predicted from impedance tube absorption data; gray curve: spectrum measured with near-grazing-incidence test).

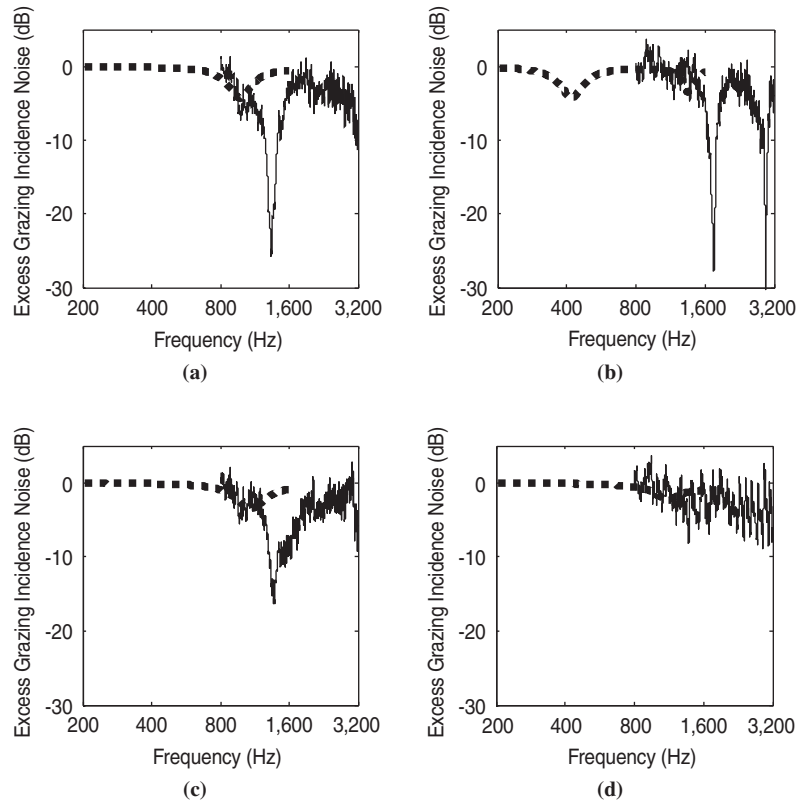


FIGURE 7 Comparison of measured (gray curve) and predicted (dotted black curve) excess near-grazing-incidence noise for representative samples from four pavement types: (a) SLP-5, (b) DLP-9, (c) TG-7, and (d) dense-graded, DG-1.

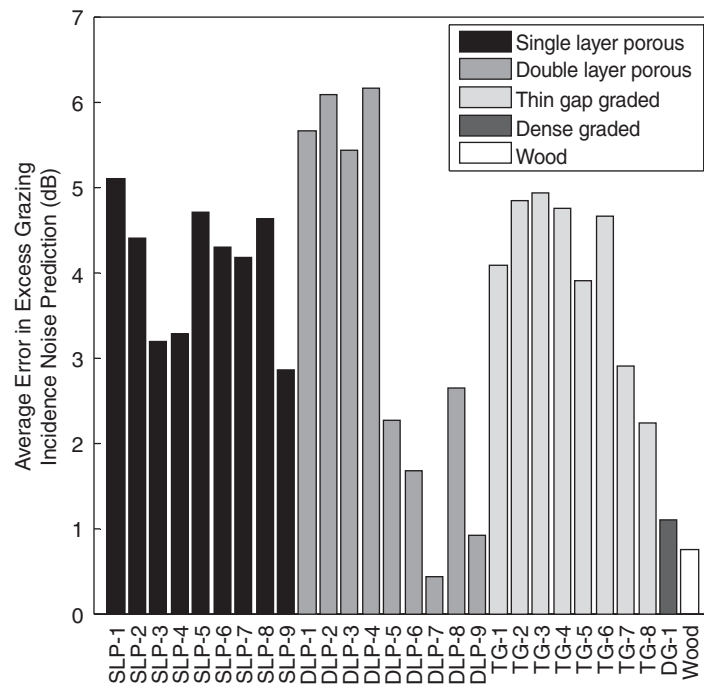


FIGURE 8 Average error in one-twelfth-octave band excess near-grazing-incidence noise prediction.

near-grazing-incidence spectra and the predictions based on absorption data is due to the sharp noise reductions caused by interference phenomena in the measured case.

DISCUSSION AND CONCLUSIONS

The results of the test for near-grazing-incidence noise reduction cannot be accurately predicted from normal incidence sound absorption data alone for porous and TG pavements. The near-grazing-incidence test gives additional information about how pavements respond to sound at shallow angles, a response which is important to TPN. Generally, the frequency of the highest reduction in near-grazing-incidence noise occurs at a higher frequency than that of the highest sound absorption, and this reduction is due to both absorption and interference.

Though the acoustical properties of a pavement cannot be fully described with a simple test, the test for near-grazing-incidence noise reduction is a simple way of obtaining additional information about the acoustic performance of pavement surfaces in the laboratory. Near-grazing-incidence information will allow more accurate comparison of onboard and pass-by measurements of TPN and will facilitate more accurate TPN prediction models.

ACKNOWLEDGMENT

This work was supported by the Federal Highway Administration, U.S. Department of Transportation.

REFERENCES

1. Crocker, M. J., D. Hanson, Z. Li, R. Karjatkar, and K. S. Vissamraju. Measurement of Acoustical and Mechanical Properties of Porous Road Surfaces and Tire and Road Noise. In *Transportation Research Record: Journal of the Transportation Research Board*, No. 1891, Transportation Research Board of the National Academies, Washington, D.C., 2004, pp. 16–22.
2. van Blokland, G., and P. The. Test Sections for Development of a Hybrid Tyre/Road Interaction Noise Model. *Proc., Inter-Noise 2007*, Istanbul, Turkey, National Research Council Canada, Ottawa, Ontario, 2007, p. 722.
3. Beckenbauer, T., P. Klein, J.-F. Hamet, and W. Kropp. Tyre/Road Noise Prediction: A Comparison Between the SPERoN and HyRoNE Models—Part 1. *Proc., Acoustics 08 Paris*, Société Française d'Acoustique, Paris, 2008, pp. 2933–2938.
4. Reyes, C. H., and J. Harvey. A Method for Predicting Sound Intensity Noise Levels Using Laboratory Pavement Cores. In *Noise-Con 2011 Proceedings* (DVD), Portland, Ore., Institute of Noise Control Engineering, Indianapolis, Ind., 2011, p. 522.
5. Ruhala, R. J., and C. B. Burroughs. Localization of Tire/Pavement Noise Source Regions. *Noise Control Engineering Journal*, Vol. 56, 2008, p. 318.
6. Donovan, P. R., and D. M. Lodico. Estimation of Vehicle Pass-By Noise Emission Levels from Onboard Sound Intensity Levels of Tire–Pavement Noise. In *Transportation Research Record: Journal of the Transportation Research Board*, No. 2123, Transportation Research Board of the National Academies, Washington, D.C., 2009, pp. 137–144.
7. Donovan, P. R. The Effects of Porous Pavements on Tire/Pavement Noise Source Levels and Pass-By Measurements. *Noise-Con 2011 Proceedings* (DVD), Portland, Ore., Institute of Noise Control Engineering, Indianapolis, Ind., 2011, p. 1244.
8. Nelson, J. T., E. Kohler, A. Ongel, and B. Rymer. Acoustical Absorption of Porous Pavement. In *Transportation Research Record: Journal of the Transportation Research Board*, No. 2058, Transportation Research Board of the National Academies, Washington, D.C., 2008, pp. 125–132.
9. Abbot, P. B., B. Andersen, F. Anfosso-Lédée, W. Bartolomaeus, H. Bendtsen, G. van Blokland, M. Eijbersen, G. Descornet, J. Ejsmont, J. Haberl, J.-F. Hamet, P. Mioduszewski, R. Nilsson, C. Padmos, E. Pucher, C. Roovers, U. Sandberg, N. Sliwa, K. Veisten, W. J. van Vliet, and G. Watts. *Guidance Manual for the Implementation of Low-Noise Road Surfaces*. Report 2006/02. Forum of European National Highway Research Laboratories, Brussels, Belgium, 2006, pp. 35–79.
10. Sandberg, U. Low Noise Road Surfaces: A State-of-the-Art Review. *Journal of Acoustical Society of Japan*, Vol. 20, 1999, pp. 1–15.
11. Rochat, J. L., and D. R. Read. Investigation of the Effects of Underlying Structures on the Noise Performance of Porous Pavements. *Noise-Con 2011 Proceedings* (DVD), Portland, Ore., Institute of Noise Control Engineering, Indianapolis, Ind., 2011.

The contents of this paper reflect the views of the authors, who are responsible for the facts and the accuracy of the data presented, and do not necessarily reflect the official views or policies of the Federal Highway Administration, nor do the contents constitute a standard, specification, or regulation.

The Transportation-Related Noise and Vibration Committee peer-reviewed this paper.